


Hysteresis of axionic charge density waves

Joan Bernabeu*

Departamento de Física de la Materia Condensada, Universidad Autónoma de Madrid, Cantoblanco, E-28049 Madrid, Spain

Alberto Cortijo[†]

Instituto de Ciencia de Materiales de Madrid (ICMM), Consejo Superior de Investigaciones Científicas (CSIC), Sor Juana Inés de la Cruz 3, 28049 Madrid, Spain

 (Received 3 June 2024; revised 17 July 2024; accepted 18 July 2024; published 1 August 2024)

Magnetic catalysis is a known proposal for inducing dynamical axionic gapped phases by means of external magnetic fields from a Weyl or Dirac semimetal phase. At finite Fermi level, the phase transition is of first-order type and the magnetic field needs to reach a critical value for the transition to take place. Using the theory of bubble nucleation, we predict the order parameter features a hysteretic behavior as a function of the external magnetic field. We also analyze the experimental consequences of this hysteretic behavior in several observables like magnetoconductivity, magnetic susceptibility, and nonlinear optical coefficients. This hysteretic behavior might serve as a fingerprint of magnetic catalysis in condensed matter systems.

DOI: [10.1103/PhysRevB.110.L081101](https://doi.org/10.1103/PhysRevB.110.L081101)

Introduction. Axion insulators are topologically nontrivial quantum states of matter characterized by a magnetoelectric term in their electromagnetic response. For time-reversal invariant topological insulators, this magnetoelectric term is a (topologically quantized) constant coefficient θ . It turns out that, being constant, this term does not modify Maxwell's equations, rendering this term unobservable. To be so, the magnetoelectric coefficient must be space and/or time dependent (axion), $\theta = \theta(t, \mathbf{r})$, as shown in Ref. [1]. There are several ways to observe a nontrivial axionic response from three-dimensional topological insulators (3DTIs): The effect of external magnetic fields, 3DTIs with magnetic surface coatings that gap the surface Dirac state. Another route is to use (time reversal) \mathcal{T} -symmetry broken Weyl semimetals, where the axion term is proportional to the separation \mathbf{b} of the Weyl nodes, $\theta(\mathbf{r}) \propto \mathbf{b} \cdot \mathbf{r}$. So far, there are scarce examples of Weyl semimetals with broken \mathcal{T} symmetry. In these cases, \mathcal{T} symmetry is broken due to some sort of antiferromagnetic ordering for $\text{Co}_3\text{Sn}_2\text{S}_2$ [2] or $\text{Mn}_2\text{Bi}_2\text{Te}_5$ [3], or the exotic role of large magnetic fluctuations in the case of EuCd_2As_2 [4]. An appealing consequence of the breakdown of the \mathcal{T} symmetry is that, in these cases, fluctuations around the order parameter might act as dynamical axions, particles hypothesized in the context of high-energy physics, that couple to electromagnetic fields through the chiral anomaly induced term in the effective electromagnetic response of these insulators, if $\theta = \mathbf{b} \cdot \mathbf{r} + \delta\theta(t, \mathbf{r})$, then, the axion mode couples to the electromagnetic fields as $\mathcal{L}_{\text{axion}} \sim \delta\theta(t, \mathbf{r}) \cdot \mathbf{E} \cdot \mathbf{B}$. In addition to the previously mentioned materials, dynamical axions have been postulated to appear in exotic charge density waves (CDW) from Weyl semimetal (WSMs) systems [5–10]. Here the CDW sliding

mode or phason plays the role of the axion and the Weyl node separation is the CDW wave vector. Two scenarios have been put forward for the axionic phase to appear. The first requires internode interactions to be strong enough so as to lead to the spontaneous symmetry breaking of the global $U(1)$ chiral symmetry [6,8]. The second introduces a strong magnetic field \mathbf{B} that aids in breaking the symmetry for weaker interactions than in the first scenario [7]. The latter case is also known as magnetic catalysis (MC) of chiral symmetry breaking [11–15] and has been extensively explored in the context of QCD in a strong magnetic field [16–25]. In the context of condensed matter physics, the magnetic field is a tuneable parameter, easier to control than fermion coupling strengths, hence MC proves a promising avenue towards observing axionic CDWs. The substantial difference between these two scenarios for the formation of axionic CDWs is the effective dimensionality in the gap equation. In the later case, the magnetic field induces the formation of (highly degenerate) $(1+1)$ -dimensional Landau level states. The resulting gap equation differs from the one in absence of magnetic field in that the solution implies a nonzero value of the chiral symmetry breaking condensate $\Delta \sim G\langle\bar{\Psi}\Psi\rangle \sim \sqrt{eB} \exp(-\frac{1}{GeB})$, for any value of the interaction constant G , while at zero magnetic field, this condensate is nonzero for values of G exceeding a critical value G_c [6]. For some specific conditions, at zero magnetic field there is the possibility of Fermi surface nesting when a chiral imbalance takes place in the WSM phase [26]. The presence of a finite chemical potential destroys this nesting condition between Fermi surfaces with opposite chirality, preventing the instability to happen for a homogeneous chiral condensate. Interestingly, it is suggested that a finite-momentum chiral condensate might be allowed in such conditions [26]. A similar situation occurs at nonzero magnetic fields. It is already known that temperature or chemical potential restores the chiral symmetry leading to a zero

*Contact author: joan.bernabeu@uam.es

†Contact author: alberto.cortijo@csic.es

value for the condensate Δ [27,28]. The salient feature, as we will discuss in the rest of this work, is that, in stark contrast to what happens at finite temperature, at finite chemical potential the effective potential for Δ develops two minima, one at $\Delta = 0$, and the other at finite values of Δ (in contrast to the $\mu = 0$ case where only $\Delta \neq 0$ is a true minimum). The presence of two minima implies that the chiral symmetry breaking phase transition is of first-order type [27]. This phase transition was analyzed in terms of varying the chemical potential at fixed magnetic field. However, in the case of three-dimensional WSMs, it is easier to knob the magnetic field instead of μ . This means that there is now a critical value for the magnetic field B_0 below which the chiral symmetry is not broken. This rather trivial conclusion might be behind the MC scenario is difficult to observe experimentally in systems with large μ . Interestingly, that this axionic CDW phase transition is of first order implies a rich structure in the dynamics of the phase transition and allows us to predict phenomenological properties that unambiguously characterize this phase transition.

Analysis of the phase transition. From a microscopic point of view, it has been suggested that electron-phonon interactions might be the primary (albeit not unique) sources of electronic correlations in WSMs [29], either in terms of a Yukawa-like (screened) coupling between acoustic phonons [30] and electrons, or interactions between electrons and optical phonons [31]. In any case, for scales smaller than the typical scale of these interactions (screening of the Yukawa interaction or energies below the optical phonon frequencies), it is sufficient with considering a contact interaction. For this reason, we will consider the standard situation of analyzing the Nambu-Jona-Lasinio (NJL) model (a local four-fermion interaction) for Dirac fermions applied to the MC scenario focusing on the infrared properties of the magnetic catalysis of the chiral symmetry. The fermionic Lagrangian of the model at finite chemical potential μ and magnetic field $\mathbf{B} = B\hat{z}$ is [27,32] reads

$$\mathcal{L}_{\text{NJL}} = \bar{\Psi}(i\gamma^\mu \eta_\mu^v D_\nu - \mu\gamma^0)\Psi - \frac{G}{2}[(\bar{\Psi}\Psi)^2 + (\bar{\Psi}i\gamma^5\Psi)^2]. \quad (1)$$

In Eq. (1) we adopt the standard quasirelativistic notation for gapless fermions in WSMs where $\eta_\mu^v = \text{diag}(-1, v_f, v_f, v_f)$, and v_f is the Fermi velocity, so the matrices γ follow the conventional Clifford algebra. We will implicitly take $v_f = 1$, reintroducing it explicitly when convenient. In addition, we define the covariant derivative as $D_\mu \equiv \partial_\mu - ieA_\mu$. We choose to represent the four-vector potential of a constant magnetic field in the x_3 direction in the symmetric gauge, i.e., $A_\mu = \frac{B}{2}(0, -x_2, x_1, 0)$. We will assume from this point on that $eB > 0$, without loss of generality.

After a Hubbard-Stratonovich transformation that transforms the quartic interaction in Eq. (1) into a bilinear interaction [14,27] with auxiliary bosonic fields Δ and θ such that $\langle \bar{\Psi}\Psi \rangle \sim \Delta \cos\theta$, and $\langle \bar{\Psi}i\gamma^5\Psi \rangle \sim \Delta \sin\theta$, one finds that, at finite temperature T and μ , the effective potential density (hereafter, effective potential) for the chiral condensate is the sum of two terms, $V(\Delta) = V_0(\Delta) + V_{\mu,T}(\Delta)$, where

$$V_0(\Delta) = \frac{\Delta^2}{2G} + \frac{eB}{8\pi^2} \int_{\Lambda^{-2}}^{\infty} \frac{ds}{s^2} e^{-s\Delta^2} \coth(eBs), \quad (2)$$

and

$$V_{\mu,T}(\Delta) = -\frac{1}{\beta} \frac{eB}{4\pi^2} \sum_{n=0}^{\infty} \alpha_n \int_{-\infty}^{\infty} dp \cdot \log\{[1 + e^{-\beta(\varepsilon_n(p)+\mu)}][1 + e^{-\beta(\varepsilon_n(p)-\mu)}]\}. \quad (3)$$

These expressions come from a standard derivation of the effective action after integrating out the electronic degrees of freedom, and under the assumption that the field Δ is constant. As usual, the field θ does not enter in this static approximation as it describes the Nambu-Goldstone mode of the transition.

The term in Eq. (2) is the vacuum contribution that is independent of T and μ , but dependent on the UV cutoff of the theory Λ . $\varepsilon_n(p) \equiv \sqrt{p^2 + 2neB + \Delta^2}$, $\alpha_n \equiv 2 - \delta_{n0}$ are the energies and degeneracies of the n Landau level, respectively, and $\beta \equiv 1/T$. Within the conventional scenario of magnetic catalysis of chiral symmetry breaking at $T = 0$, $\mu = 0$, the minimum of $V(\Delta)$ takes a nonzero value Δ_0 (corresponding to the symmetry broken phase) for any nonzero magnetic field and any $G > 0$, hence inducing a gap in the single-particle spectrum (for details of the gap equation at zero and finite μ , see Ref. [33]). In contrast, in the limit of vanishing magnetic field, a nonzero gap is only reached for couplings above a critical value $G > G_c = \frac{4\pi^2}{\Lambda^2}$. Redefining the coupling constant through the dimensionless parameter $g \equiv \frac{\Lambda^2 G}{4\pi^2}$, this bound conveniently becomes $g > 1$.

There are some qualitative features from the physics of phase transitions that we can draw from Eqs. (2) and (3). Increasing the temperature T from zero but keeping $\mu = 0$, there is a second-order (continuous) phase transition at $T \sim \Delta_0$ to the chirally symmetric phase [15,27,34]. On the other hand, increasing μ but keeping $T = 0$, one finds there is a first-order phase transition for $\mu \sim \Delta_0$. In this regime, the potential (3) takes the form

$$V_{\mu,0}(\Delta) = -\frac{eB}{4\pi^2} \sum_{n=0}^{\infty} \alpha_n \int_{-\infty}^{\infty} dp \Theta[\mu - \varepsilon_n(p)] \cdot [\mu - \varepsilon_n(p)]. \quad (4)$$

where $\Theta[x]$ is the Heaviside step function.

For the rest of the present work, we will focus on this quantum regime, $T = 0$. The full potential $V(\Delta)$ as a function of the order parameter Δ at zero temperature but a fixed value of μ is plotted in Fig. 1(a) for different values of the magnetic field. The main feature is that two minima coexist for a range of magnetic fields. The critical magnetic field B_0 is defined as the magnetic field for which the potential minima are degenerate. In addition, we can define two values of the magnetic fields B_a and B_b for which one of the minima disappear: $\frac{d^2V}{d\Delta^2}|_{B=B_{a,b}} = 0$ (the symmetric minimum around $\Delta = 0$ and the symmetry-breaking minimum at $\Delta \neq 0$, respectively). For magnetic fields B larger than B_b (smaller than B_a), the symmetric (symmetry-breaking) minimum becomes *unstable*. For $B_a < B < B_0$ ($B_b > B > B_0$), the chirality-symmetric (chirality-breaking) minimum is the global minimum, i.e., the *stable* ground state. It is well known that for sufficiently small perturbations around B_0 whereby the ground state of the system passes from lying at the global minimum to simply a local one, the system remains in its original, now

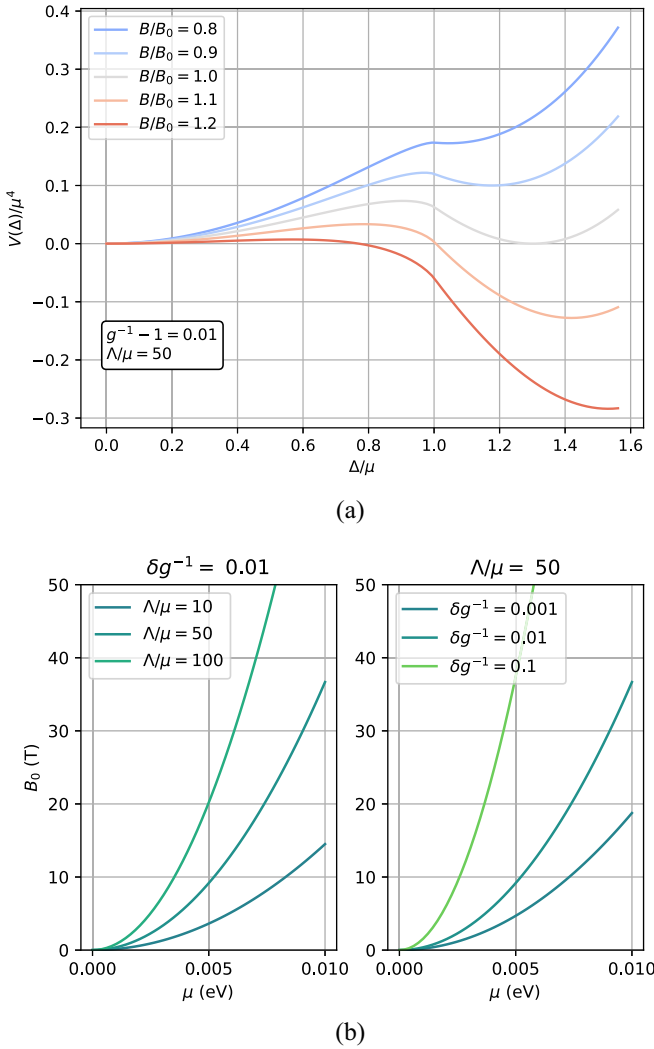


FIG. 1. (a) Plot of $V(\Delta)$ for different magnetic fields, referenced with respect to the degeneracy value B_0 , where two minima coexist, with $\Lambda = 50\mu$ and $\delta g^{-1} \equiv g^{-1} - 1 \equiv \frac{\Lambda^2 G}{4\pi^2} - 1 = 0.01$. (b) Plot of the value of the critical field B_0 as a function of the chemical potential for varying values of Λ/μ with fixed $g^{-1} - 1 = 0.01$ (left) and varying values of $g^{-1} - 1$ with fixed $\Lambda/\mu = 50$ (right). Note that throughout this work values of g are referenced with respect to its critical value $g_c = 1$ in the NJL model, as this is where the interaction gap becomes prominent [14], and is displayed in the right plot of (b).

metastable, ground state [35]. In thermal (i.e., temperature-driven) first-order phase transitions this phenomenon is known as supercooling (for temperatures T smaller than a critical temperature T_0) and superheating (for $T > T_0$). However, the system might transition into the true global minimum well by some external perturbation (or thermal fluctuations in thermal phase transitions), or spontaneously at some values of the magnetic field, B_1 and B_2 , (or any external knob parameter) with $B_a \leq B_1 \leq B_0 \leq B_2 \leq B_b$. In the case where B_1 and/or B_2 are different from B_0 , and the transition takes place dynamically by nucleation of bubbles [36,37], the phase transition will show a hysteretic behavior [38].

All these considerations are generic of first-order phase transitions [35]. In our particular case, the effective potential

arises from the pseudorelativistic interacting electrons described by the model in Eq. (1), so it is worth highlighting the formal similarity of this model with the ones studied in the context of cosmological phase transitions [39–42]. Those transitions are often characterized by a symmetry-preserving phase at high temperatures. As the universe expands, it cools down and the temperature is lowered until the symmetry-broken phase becomes energetically favorable at a certain critical temperature T_0 . If this transition is thermal and of first order, then for temperatures immediately below T_0 , the universe will stay in its original but now metastable symmetry-preserving phase. This will occur until bubbles of the symmetry-breaking phase nucleate and expand until they occupy the entire volume of the universe. In these models the nucleation rate Γ is given by the high-temperature Arrhenius-like dependence $\Gamma \propto e^{-\Delta F/T}$ [40,43,44]. This is in contrast to the quantum scenario considered here, where, as was argued previously, the first-order phase transition was observed when the temperature is the smallest energy scale $T \ll \mu, \sqrt{eB}, \Lambda$. The relevant nucleation rate is then given by the semiclassical expression for Γ [36,37],

$$\Gamma \approx \left(\frac{S_b}{2\pi R_b^2} \right)^2 e^{-S_b}, \quad (5)$$

where S_b is the action for the classical bubble solution to the equations of motion in four-dimensional (4D) Euclidean space (that will be specified later), and R_b is the radius of the bubble. Another important difference with respect to cosmological phase transitions is that the transition-driving parameter, the magnetic field B , can be lowered or raised in a controlled fashion in the experiment. Hence, the transition from the chirality-breaking to the chirality-preserving phase might be tuned as the nucleation rate Γ will depend on the magnetic field. If the system parameters are such that (B_1, B_2) are different enough from B_0 , the hysteretic behavior might be observed experimentally. In the following sections we will first estimate the values of B_1 and B_2 using a modified version of the theory of bubble nucleation and later we will compute several observables where this hysteretic behavior can be measured.

Calculation of the Nucleation Rate. To find the magnetic fields B_1 and B_2 on either side of B_0 for which the material effectively transitions, we calculate the time a critical bubble takes to nucleate [42,45], defined by $t_{\text{nuc}}^{-1} \sim R_b^3 \Gamma$. We assume that, due to fast expansion of the bubble at speeds approaching v_f , the whole sample transitions once a single bubble nucleates. From this perspective, the transition from the symmetric to the broken phase happens at $t_{\text{nuc}}(B_2) < t_r$, where t_r is some time reference scale much longer than any set in an experiment. Similarly, the magnetic field for which the transition from the broken to the symmetric field occurs B_1 is set by $t_{\text{nuc}}(B_1) < t_r$. We will consider the conservative $t_r = 10^9$ years. As will be checked later, B_1 and B_2 are not too sensitive to smaller, perhaps more sensible, values of t_r .

To calculate the bubble configuration, we need to take into account kinetic effects beyond the static potential $V(\Delta)$ in Eqs. (2) and (3). This approach has been used, for instance, to calculate the bubble configurations of first-order chiral phase

transition of the early universe [46]. Keeping the leading terms in the corresponding derivative expansion of the effective action, the kinetic terms for the condensate read

$$\mathcal{L}_k = \frac{Z^{-1}(\Delta)}{2} \left[(\partial_0 \Delta)^2 - \sum_i v_i^2 (\partial_i \Delta)^2 \right]. \quad (6)$$

To recover a canonical $O(4)$ -symmetric kinetic term, we introduce a new field Φ defined by

$$\frac{d\Phi}{d\Delta} = Z^{-\frac{1}{2}}(\Delta), \quad (7)$$

and assume for the sake of simplicity that the velocity of the bosons in the plane perpendicular to the magnetic field $v_\perp = v_1 = v_2$ of the Δ bosons is equal to the longitudinal velocity, the Fermi velocity v_f . This is generally not the case [14,47] as clearly the magnetic field breaks rotation symmetry, but is justified for the cases considered here where the symmetry-breaking ground state $\Delta_0 \sim \mu$ is not extremely small compared to Λ and the magnetic field is in a nonultra-quantum regime $eB \ll \Lambda^2$ [48]. The field renormalization can be calculated from

$$\begin{aligned} Z^{-1}(\Delta) &= \frac{i}{2} \int \frac{d^4k}{(2\pi)^4} \text{tr} \left[\frac{\partial \tilde{\mathcal{D}}}{\partial k_0} \frac{\partial \tilde{\mathcal{D}}}{\partial k_0} \right] \\ &= \frac{eB}{24\pi^2 \Delta^2} \left[1 - \left(1 - \frac{\Delta^2}{\mu^2} \right)^{\frac{3}{2}} \Theta(\mu - \Delta) \right], \end{aligned} \quad (8)$$

where $\tilde{\mathcal{D}}$ is the translation-invariant component of the lowest Landau level (LLL) propagator in momentum space [14]

$$\tilde{\mathcal{D}}(k) = i \exp \left[-\frac{\mathbf{k}_\perp^2}{eB} \right] \frac{k_\parallel + \Delta}{k_\parallel^2 - \Delta^2} (1 - i\gamma^1 \gamma^2), \quad (9)$$

and $k \equiv (k_0, k_1, k_2, k_3)$, $\mathbf{k}_\perp \equiv (k_1, k_2)$, and $k_\parallel \equiv (k_0, k_3)$. Notice how the μ -dependent term makes the field renormalization finite even in the limit $\Delta \rightarrow 0$, which would otherwise diverge in the $\mu = 0$ case [14]. It is therefore essential for this term to be included, as otherwise if such a divergence were left unabated, then the gapless ground state of $V(\Phi)$ would be found at $\Phi \rightarrow \infty$ and would inhibit any stable bubble configuration with a metastable gapless configuration.

The bubble configurations for different values of the magnetic field can now be obtained solving the equation of motion of the canonical field with respect to the radial coordinate ρ , i.e.,

$$\frac{d^2\Phi}{d\rho^2} + \frac{3}{\rho} \frac{d\Phi}{d\rho} = Z^{\frac{1}{2}} \frac{dV}{d\Delta}, \quad (10)$$

imposing the conditions $\lim_{\rho \rightarrow \infty} \Phi = \Phi_{\text{meta}}$, where Φ_{meta} denotes the corresponding metastable state, and $d\Phi/d\rho|_{\rho=0} = 0$, using an undershooting-overshooting algorithm (see, e.g., Ref. [49]). These bubble solutions are then used to calculate the corresponding bubble action

$$S_b = \int d^4x \left[\frac{1}{2} (\nabla\Phi)^2 + V(\Phi) - V(\Phi_{\text{meta}}) \right]. \quad (11)$$

The resulting nucleation times are plotted in Fig. 2. The curves have a steep descent as they approach B_0 , so much so that lowering t_r down to 10^3 years, for instance, would not alter

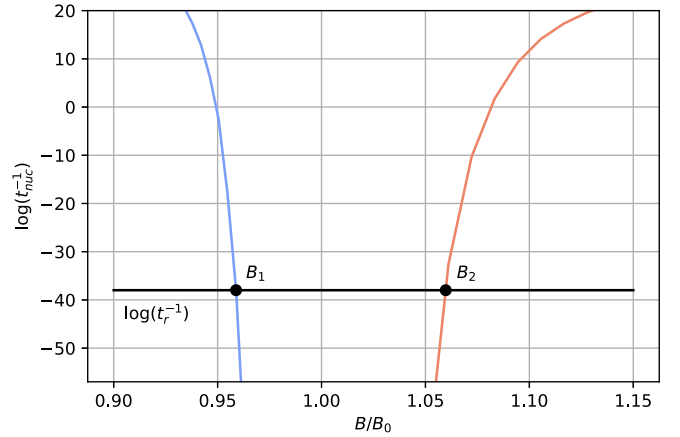


FIG. 2. Plot of the logarithm of the inverse nucleation time t_{nuc}^{-1} (measured in inverse seconds) for different magnetic fields, compared with the reference time $t_r = 10^9$ years, with $g^{-1} - 1 \equiv \frac{\Lambda^2 G}{4\pi^2} - 1 = 0.01$, $\Lambda = 50\mu$, and $\mu = 0.01$ eV.

the values of B_1 and B_2 significantly. Having determined the points at which the phase transition occurs, one can now draw hysteresis curves for gap-dependent quantities.

Observable consequences. In Figs. 3(a) to 3(c) we plot the hysteresis curves for the gap, the magnetoconductivity in the quantum limit [50], and the magnetic susceptibility [7,51]. Although the model predicts that the system should remain conducting even in the gapped phase because of the surviving Nambu-Goldstone boson, the axion, the associated charge density wave is expected to be pinned if no depinning potential is applied [52]. This is the case represented in Fig. 3(b).

In addition, we also consider the effects of hysteresis in nonlinear optical response. Since in our model (1) the Weyl nodes are located at the same energy, the second-order response is null. Therefore, we consider the third-order response, particularly the component σ^{zzzz} at third harmonic generation, where all incident photons have the same frequency ω [53] and are parallel to the applied magnetic field. The contribution of the LLL, of interest in the magnetic catalysis scenario, is

$$\begin{aligned} \sigma^{zzzz}(\omega, \omega, \omega) &= (ev_f)^4 \frac{1}{3!} \frac{eB}{4\pi^2} \int_{-\infty}^{\infty} dp \\ &\times \frac{2^7 \Delta^2 (4\varepsilon_0^2(p) - 5\Delta^2 + \omega^2)}{\varepsilon_0(p) [9\omega^6 - 49\varepsilon_0^2(p)\omega^4 + 56\varepsilon_0^4(p)\omega^2 - 16\varepsilon_0^6(p)]}. \end{aligned} \quad (12)$$

Note that the denominator can be decomposed into poles around $\omega = \pm 2\Delta/n$ where $n = 1, 2, 3$. This response function is a sensitive probe to the phase transition as it is zero in the gapless phase. This is fundamentally a consequence of the one-dimensional (1D) LLL dynamics and indeed it can be checked that it is nonzero in a Weyl SM or graphene [54] in the absence of a magnetic field. Therefore, as the magnetic field is turned on and increased, one expects to see a gradual decline of σ^{zzzz} during the quantum oscillating region until acquiring a minimal value in the quantum limit. However, once the phase

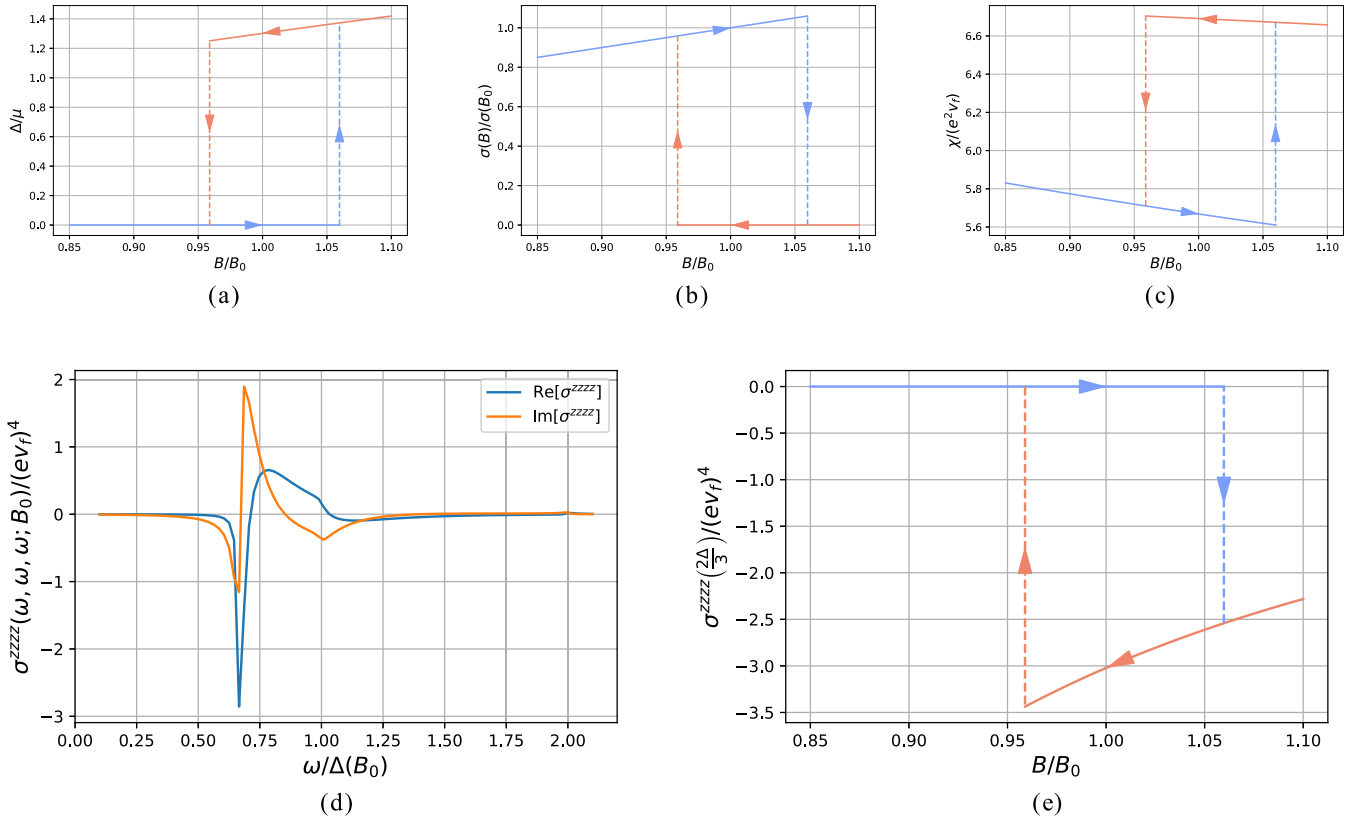


FIG. 3. Hysteresis diagrams of the (a) gap, (b) the magnetoconductivity, and (c) the magnetic susceptibility. (d) Plot of the third harmonic optical magnetoconductivity component σ^{zzzz} at $B = B_0$. The strong peak corresponds to $\omega = 2\Delta/3$. A broadening of $\eta = 0.01\mu$ (such that $\omega \rightarrow \omega + i\eta$) is employed. (e) Hysteresis diagram of σ^{zzzz} evaluated at $3\omega = 2\Delta(B)$. In all plots the parameter values $g^{-1} - 1 = 0.01$, $\Lambda = 50\mu$, and $\mu = 0.01$ eV are used.

transition occurs at B_2 , it will become finite in the gapped phase, as is represented in Fig. 3(d). The most prevalent feature is the peak at $3\omega = 2\Delta$ in the real part. The hysteresis plot for σ^{zzzz} at this frequency is represented in Fig. 3(e).

The dependence of the critical field B_0 on the model parameters is explored in Fig. 1(b). Curves for B_1 and B_2 are not shown but it has been checked that they follow analogous curves [33], and hence the size of the hysteresis window relative to B_0 shown in Fig. 3 is relatively unchanged. The hysteresis process is accessible for small chemical potentials, as this is when the contribution from the LLL (see, again, Ref. [33]), the key piece in inducing MC, is most relevant. In addition, near-critical couplings g and not so large UV scales Λ also favor the process occurring at realistic scales for the magnetic field, as is generally expected in MC [7]. It is worth pointing out however that in the ultraquantum limit $\Lambda^2 \ll eB$, no hysteresis should be observed as in that limit the process is independent of the value of the magnetic field modulus [48].

Conclusions. The present work highlights the fact that a first-order phase transition for the magnetic catalysis scenario implies, first, the existence of a chemical potential-dependent critical magnetic field B_0 below which the transition cannot take place, and second, a hysteretic behavior in the condensate as a function of the magnetic field, and thus the existence of hysteresis loops in the physical observables that depend on the condensate, that is only compatible with the effect of many-

body interactions. We show that a hysteretic process should indeed be observable, as the transition values of the magnetic field, B_1 and B_2 , are well distinguished from one another. The way in which disorder may alter this conclusion remains to be studied in future work. However, it is reasonable to expect it to slow nucleation, and hence widen the hysteretic window, as is the case with $1 + 0D$ quantum tunneling [55].

From an experimental perspective in the field of WSMs, the magnetic field-induced axionic phase has been reported in $(\text{TaSe}_4)_2\text{I}$ [52]. Transport measurements in materials in CDW states can, however, be difficult to interpret due to the Joule heating associated to the voltage to depin the sliding mode [56]. Also, a metal-insulator transition driven by external magnetic fields, compatible with the MC scenario, were claimed to be observed for the case of ZrTe_5 and HfTe_5 [57–60]. This point of view has been later disputed in ZrTe_5 [61], where no signatures of an electron instability were found, and a conclusive experimental situation for these compounds is still missing. The presence of hysteresis loops in experimental observables might be a conclusive fingerprint of many-body instabilities versus single-particle effects.

As a final remark, we note that the pseudorelativistic theory presented here can be viewed as a condensed matter analog [62] of a cosmological chiral phase transition [41,42], with the notable difference that the tuning parameter for the transition is the magnetic field and not the temperature of the expanding universe.

Acknowledgments. J.B. is supported by FPU Grant No. FPU20/01087. A.C. acknowledges financial support from the Ministerio de Ciencia e Innovación through the Grant No. PID2021-127240NB-I00. J.B. and A.C.

acknowledge discussions with M. A. H. Vozmediano, M. Tolosa-Simeón, B. Hawashin, and M. M. Scherer, J. J. Esteve-Paredes, A. J. Uría-Álvarez, M. A. García-Blazquez, and J. J. Palacios.

-
- [1] F. Wilczek, Two applications of axion electrodynamics, *Phys. Rev. Lett.* **58**, 1799 (1987).
- [2] Y. Okamura, S. Minami, Y. Kato, Y. Fujishiro, Y. Kaneko, J. Ikeda, J. Muramoto, R. Kaneko, K. Ueda, V. Kocsis, N. Kanazawa, Y. Taguchi, T. Koretsune, K. Fujiwara, A. Tsukazaki, R. Arita, Y. Tokura, and Y. Takahashi, Giant magneto-optical responses in magnetic Weyl semimetal $\text{Co}_3\text{Sn}_2\text{S}_2$, *Nat. Commun.* **11**, 4619 (2020).
- [3] J. Zhang, D. Wang, M. Shi, T. Zhu, H. Zhang, and J. Wang, Large dynamical axion field in topological antiferromagnetic insulator $\text{Mn}_2\text{Bi}_2\text{Te}_5$, *Chin. Phys. Lett.* **37**, 077304 (2020).
- [4] J.-Z. Ma, S. M. Nie, C. J. Yi, J. Jandke, T. Shang, M. Y. Yao, M. Naamneh, L. Q. Yan, Y. Sun, A. Chikina, V. N. Strocov, M. Medarde, M. Song, Y.-M. Xiong, G. Xu, W. Wulfhekkel, J. Mesot, M. Reticcioli, C. Franchini, C. Mudry *et al.*, Spin fluctuation induced Weyl semimetal state in the paramagnetic phase of EuCd_2As_2 , *Sci. Adv.* **5**, eaaw4718 (2019).
- [5] R. Li, J. Wang, X.-L. Qi, and S.-C. Zhang, Dynamical axion field in topological magnetic insulators, *Nat. Phys.* **6**, 284 (2010).
- [6] Z. Wang and S.-C. Zhang, Chiral anomaly, charge density waves, and axion strings from Weyl semimetals, *Phys. Rev. B* **87**, 161107(R) (2013).
- [7] B. Roy and J. D. Sau, Magnetic catalysis and axionic charge density wave in Weyl semimetals, *Phys. Rev. B* **92**, 125141 (2015).
- [8] B. Roy, P. Goswami, and V. Juričić, Interacting Weyl fermions: Phases, phase transitions, and global phase diagram, *Phys. Rev. B* **95**, 201102(R) (2017).
- [9] D. Sehayek, M. Thakurathi, and A. A. Burkov, Charge density waves in Weyl semimetals, *Phys. Rev. B* **102**, 115159 (2020).
- [10] B. J. Wieder, K.-S. Lin, and B. Bradlyn, Axionic band topology in inversion-symmetric Weyl-charge-density waves, *Phys. Rev. Res.* **2**, 042010(R) (2020).
- [11] K. G. Klimenko, Three-dimensional Gross-Neveu model in an external magnetic field. I, *Theor. Math. Phys.* **89**, 1161 (1991).
- [12] K. G. Klimenko, Three-dimensional Gross-Neveu model in an external electric field. II, *Theor. Math. Phys.* **89**, 1287 (1991).
- [13] V. P. Gusynin, V. A. Miransky, and I. A. Shovkovy, Catalysis of dynamical flavor symmetry breaking by a magnetic field in $2 + 1$ dimensions, *Phys. Rev. Lett.* **73**, 3499 (1994).
- [14] V. Gusynin, V. Miransky, and I. Shovkovy, Dimensional reduction and dynamical chiral symmetry breaking by a magnetic field in $3+1$ dimensions, *Phys. Lett. B* **349**, 477 (1995).
- [15] V. A. Miransky and I. A. Shovkovy, Quantum field theory in a magnetic field: From quantum chromodynamics to graphene and dirac semimetals, *Phys. Rep.* **576**, 1 (2015).
- [16] S. P. Klevansky and R. H. Lemmer, Chiral-symmetry restoration in the Nambu–Jona-Lasinio model with a constant electromagnetic field, *Phys. Rev. D* **39**, 3478 (1989).
- [17] H. Suganuma and T. Tatsumi, On the behavior of symmetry and phase transitions in a strong electromagnetic field, *Ann. Phys. (NY)* **208**, 470 (1991).
- [18] S. Schramm, B. Müller, and A. J. Schramm, Quark-antiquark condensates in strong magnetic fields., *Mod. Phys. Lett. A* **07**, 973 (1992).
- [19] D. Kabat, K. Lee, and E. Weinberg, QCD vacuum structure in strong magnetic fields, *Phys. Rev. D* **66**, 014004 (2002).
- [20] V. A. Miransky and I. A. Shovkovy, Magnetic catalysis and anisotropic confinement in QCD, *Phys. Rev. D* **66**, 045006 (2002).
- [21] P. Buividovich, M. Chernodub, E. Luschevskaya, and M. Polikarpov, Numerical study of chiral symmetry breaking in non-Abelian gauge theory with background magnetic field, *Phys. Lett. B* **682**, 484 (2010).
- [22] M. D’Elia, S. Mukherjee, and F. Sanfilippo, QCD phase transition in a strong magnetic background, *Phys. Rev. D* **82**, 051501(R) (2010).
- [23] M. D’Elia and F. Negro, Chiral properties of strong interactions in a magnetic background, *Phys. Rev. D* **83**, 114028 (2011).
- [24] G. S. Bali, F. Bruckmann, G. Endrődi, Z. Fodor, S. D. Katz, S. Krieg, A. Schäfer, and K. K. Szabó, The QCD phase diagram for external magnetic fields, *J. High Energy Phys.* **02** (2012) 044.
- [25] G. S. Bali, F. Bruckmann, G. Endrődi, Z. Fodor, S. D. Katz, and A. Schäfer, QCD quark condensate in external magnetic fields, *Phys. Rev. D* **86**, 071502(R) (2012).
- [26] J. B. Curtis, I. Petrides, and P. Narang, Finite-momentum instability of a dynamical axion insulator, *Phys. Rev. B* **107**, 205118 (2023).
- [27] D. Ebert, K. G. Klimenko, M. A. Vdovichenko, and A. S. Vshivtsev, Magnetic oscillations in dense cold quark matter with four-fermion interactions, *Phys. Rev. D* **61**, 025005 (1999).
- [28] K. Fukushima and J. M. Pawłowski, Magnetic catalysis in hot and dense quark matter and quantum fluctuations, *Phys. Rev. D* **86**, 076013 (2012).
- [29] P.-L. Zhao, H.-Z. Lu, and X. C. Xie, Theory for magnetic-field-driven 3D metal-insulator transitions in the quantum limit, *Phys. Rev. Lett.* **127**, 046602 (2021).
- [30] F. Qin, S. Li, Z. Z. Du, C. M. Wang, W. Zhang, D. Yu, H.-Z. Lu, and X. C. Xie, Theory for the charge-density-wave mechanism of 3D quantum Hall effect, *Phys. Rev. Lett.* **125**, 206601 (2020).
- [31] S. Kundu, C. Bourbonnais, and I. Garate, Theory of phonon instabilities in Weyl semimetals at high magnetic fields, *Phys. Rev. B* **105**, 195113 (2022).
- [32] M. Vdovichenko, A. Vshivtsev, and K. Klimenko, Magnetic catalysis and magnetic oscillations in the Nambu–Jona-Lasinio model, *Phys. At. Nucl.* **63**, 470 (2000).
- [33] See Supplemental Material at <http://link.aps.org/supplemental/10.1103/PhysRevB.110.L081101> for details of the minima structure of the effective potential at finite chemical potential μ , and further details of the dependence of B_0 , B_1 , and B_2 with the coupling constant g , the cutoff Λ , and the chemical potential μ .

- [34] D.-S. Lee, C. N. Leung, and Y. J. Ng, Chiral symmetry breaking in a uniform external magnetic field. II. Symmetry restoration at high temperatures and chemical potentials, *Phys. Rev. D* **57**, 5224 (1998).
- [35] K. Binder, Theory of first-order phase transitions, *Rep. Prog. Phys.* **50**, 783 (1987).
- [36] S. Coleman, Fate of the false vacuum: Semiclassical theory, *Phys. Rev. D* **15**, 2929 (1977).
- [37] C. G. Callan and S. Coleman, Fate of the false vacuum. II. First quantum corrections, *Phys. Rev. D* **16**, 1762 (1977).
- [38] G. S. Agarwal and S. R. Shenoy, Observability of hysteresis in first-order equilibrium and nonequilibrium phase transitions, *Phys. Rev. A* **23**, 2719 (1981).
- [39] A. D. Linde, Phase transitions in gauge theories and cosmology, *Rep. Prog. Phys.* **42**, 389 (1979).
- [40] A. Linde, Decay of the false vacuum at finite temperature, *Nucl. Phys. B* **216**, 421 (1983).
- [41] L. P. Csernai and J. I. Kapusta, Nucleation of relativistic first-order phase transitions, *Phys. Rev. D* **46**, 1379 (1992).
- [42] L. P. Csernai and J. I. Kapusta, Dynamics of the QCD phase transition, *Phys. Rev. Lett.* **69**, 737 (1992).
- [43] J. Langer, Statistical theory of the decay of metastable states, *Ann. Phys. (NY)* **54**, 258 (1969).
- [44] I. Affleck, Quantum-statistical metastability, *Phys. Rev. Lett.* **46**, 388 (1981).
- [45] J. S. Langer and A. J. Schwartz, Kinetics of nucleation in near-critical fluids, *Phys. Rev. A* **21**, 948 (1980).
- [46] M. Aoki, H. Goto, and J. Kubo, Gravitational waves from hidden QCD phase transition, *Phys. Rev. D* **96**, 075045 (2017).
- [47] K. Fukushima and Y. Hidaka, Magnetic catalysis versus magnetic inhibition, *Phys. Rev. Lett.* **110**, 031601 (2013).
- [48] J. Bernabeu and A. Cortijo, Chiral symmetry restoration and the ultraquantum limit of axionic charge density waves in Weyl semimetals, *J. High Energy Phys.* **03** (2024) 126.
- [49] R. Apreda, M. Maggiore, A. Nicolis, and A. Riotto, Gravitational waves from electroweak phase transitions, *Nucl. Phys. B* **631**, 342 (2002).
- [50] D. T. Son and B. Z. Spivak, Chiral anomaly and classical negative magnetoresistance of Weyl metals, *Phys. Rev. B* **88**, 104412 (2013).
- [51] P. Goswami and S. Chakravarty, Quantum criticality between topological and band insulators in $3 + 1$ dimensions, *Phys. Rev. Lett.* **107**, 196803 (2011).
- [52] J. Gooth, B. Bradlyn, S. Honnali, C. Schindler, N. Kumar, J. Noky, Y. Qi, C. Shekhar, Y. Sun, Z. Wang, B. A. Bernevig, and C. Felser, Axionic charge-density wave in the Weyl semimetal $(\text{TaSe}_4)_2\text{I}$, *Nature (London)* **575**, 315 (2019).
- [53] D. E. Parker, T. Morimoto, J. Orenstein, and J. E. Moore, Diagrammatic approach to nonlinear optical response with application to Weyl semimetals, *Phys. Rev. B* **99**, 045121 (2019).
- [54] D. J. Passos, G. B. Ventura, J. M. Viana Parente Lopes, J. M. B. Lopes dos Santos, and N. M. R. Peres, Nonlinear optical responses of crystalline systems: Results from a velocity gauge analysis, *Phys. Rev. B* **97**, 235446 (2018).
- [55] A. O. Caldeira and A. J. Leggett, Influence of dissipation on quantum tunneling in macroscopic systems, *Phys. Rev. Lett.* **46**, 211 (1981).
- [56] A. Sinchenko, R. Ballou, J.-E. Lorenzo, T. Grenet, and P. Monceau, Does $(\text{TaSe}_4)_2\text{I}$ really harbor an axionic charge density wave? *Appl. Phys. Lett.* **120**, 063102 (2022).
- [57] Y. Liu, X. Yuan, C. Zhang, Z. Jin, A. Narayan, C. Luo, Z. Chen, L. Yang, J. Zou, X. Wu, S. Sanvito, Z. Xia, L. Li, Z. Wang, and F. Xiu, Zeeman splitting and dynamical mass generation in Dirac semimetal ZrTe_5 , *Nat. Commun.* **7**, 12516 (2016).
- [58] F. Tang, Y. Ren, P. Wang, R. Zhong, J. Schneeloch, S. A. Yang, K. Yang, P. A. Lee, G. Gu, Z. Qiao, and L. Zhang, Three-dimensional quantum Hall effect and metal-insulator transition in ZrTe_5 , *Nature (London)* **569**, 537 (2019).
- [59] P. Wang, Y. Ren, F. Tang, P. Wang, T. Hou, H. Zeng, L. Zhang, and Z. Qiao, Approaching three-dimensional quantum Hall effect in bulk HfTe_5 , *Phys. Rev. B* **101**, 161201(R) (2020).
- [60] S. Galeski, X. Zhao, R. Wawrzyńczak, T. Meng, T. Förster, P. M. Lozano, S. Honnali, N. Lamba, T. Ehmcke, A. Markou, Q. Li., G. Gu, W. Zhu, J. Wosnitza, C. Felser, G. F. Chen, and J. Gooth, Unconventional Hall response in the quantum limit of HfTe_5 , *Nat. Commun.* **11**, 5926 (2020).
- [61] S. Galeski, T. Ehmcke, R. Wawrzyńczak, P. M. Lozano, K. Cho, A. Sharma, S. Das, F. Küster, P. Sessi, M. Brando, R. Kuchler, A. Markou, M. König, P. Swekis, C. Felser, Y. Sassa, Q. Li, G. Gu, M. V. Zimmermann, O. Ivashko *et al.*, Origin of the quasi-quantized Hall effect in ZrTe_5 , *Nat. Commun.* **12**, 3197 (2021).
- [62] C. Barcelo, S. Liberati, and M. Visser, Analogue gravity, *Living Rev. Relativity* **14**, 3 (2011).